



Agreement between numerical integration techniques during countermovement jumps with accentuated eccentric loading in youth athletes

Thomas E. Bright, Jason Lake, John R. Harry, Mia Hite, Anton Simms, Nicola Theis, Peter Mundy & Jonathan D. Hughes

To cite this article: Thomas E. Bright, Jason Lake, John R. Harry, Mia Hite, Anton Simms, Nicola Theis, Peter Mundy & Jonathan D. Hughes (29 Jun 2025): Agreement between numerical integration techniques during countermovement jumps with accentuated eccentric loading in youth athletes, Journal of Sports Sciences, DOI: [10.1080/02640414.2025.2526297](https://doi.org/10.1080/02640414.2025.2526297)

To link to this article: <https://doi.org/10.1080/02640414.2025.2526297>



© 2025 The Author(s). Published by Informa UK Limited, trading as Taylor & Francis Group.



Published online: 29 Jun 2025.



Submit your article to this journal [↗](#)



Article views: 288



View related articles [↗](#)



View Crossmark data [↗](#)

Agreement between numerical integration techniques during countermovement jumps with accentuated eccentric loading in youth athletes

Thomas E. Bright^{a,b}, Jason Lake^c, John R. Harry^d, Mia Hite^d, Anton Simms^d, Nicola Theis^e, Peter Mundy^f and Jonathan D. Hughes^a

^aYouth Physical Development Centre, Cardiff School of Sport and Health Sciences, Cardiff Metropolitan University, Cardiff, UK; ^bSchool of Sport, Exercise and Rehabilitation, Plymouth Marjon University, Plymouth, UK; ^cInstitute of Sport, Nursing, and Allied Health, University of Chichester, Chichester, UK; ^dHuman Performance & Biomechanics Laboratory, Department of Kinesiology & Sport Management, Texas Tech University, Lubbock, Texas, USA; ^eSchool of Sport and Exercise, University of Gloucestershire, Gloucester, UK; ^fHawkin Dynamics, Inc., Westbrook, Maine, USA

ABSTRACT

This study evaluated agreement between a) force platform numerical integration techniques for calculating performance variables and b) three-dimensional (3D) motion capture and vertical ground reaction force (vGRF) methods for identifying the dumbbell release during countermovement jumps with accentuated eccentric loading (CMJ_{AEL}). Twenty adolescent participants (10 males, 10 females) performed CMJ_{AEL} with handheld dumbbells at 20%, 25% and 30% of body mass. Variables were compared across five integration methods using repeated measures Bland-Altman and two-way repeated measures ANOVA analyses ($\alpha = 0.05$), with combined forward and backward integration serving as the criterion. Backward integration and after adjusting at the dumbbells release agreed with the criterion, while forward integration and adjusting at the bottom position did not. The dumbbell release point identified using 3D motion capture (criterion) was also compared to estimates derived from force platform data (vGRF method). The vGRF method identified the dumbbell release point in delay of 3D motion capture, with limits of agreement (LOA) between -0.17 and 0.03 s across conditions. These methods should not be used interchangeably; rather, we recommend that the vGRF method be used in situations whereby only force platforms are available, and that it is combined with forward and backward integration techniques.

ARTICLE HISTORY

Received 28 November 2024
Accepted 22 June 2025

KEYWORDS



Numerical integration; jumping; accentuated eccentric loading; eccentric training; youth athlete

Introduction

The countermovement jump (CMJ) is frequently used in youth strength and conditioning (S&C) programmes and testing batteries due to its ease of administration and relevance to high-intensity sporting actions. For example, jump height has shown moderate to strong correlations with 505 change of direction performance in female academy netball players ($r = -0.60$ to -0.71 ; $p < 0.01$) (Thomas et al., 2017) and sprint times over 30–60 m in elite young male sprinters ($r = -0.54$ to -0.76 ; $p < 0.05$) (Washif & Kok, 2022). During such actions, maximising the force that can be applied in the available time is critical and is largely dependent on the effective use of the stretch-shortening cycle (SSC) through a coupled eccentric-concentric muscle action (Malisoux et al., 2006). Although the ability to utilise the SSC in movements such as the CMJ develops naturally with growth and maturation (Dantas et al., 2020; Gillen et al., 2022; Pedley et al., 2022), ample evidence suggests that it can

be further augmented with relevant training methods, including resistance and plyometric training (Asadi et al., 2018; Ramirez-Campillo et al., 2023). Therefore, refining our understanding of these training methods would be beneficial for S&C coaches and practitioners who work with youth athletes.

Accentuated eccentric loading (AEL) is a training method that has been shown to enhance force output in exercises that are regulated by the SSC (Aboodarda et al., 2013; Harrison et al., 2019; Lloyd et al., 2022; Taber et al., 2023). When applied to a countermovement jump (i.e., CMJ_{AEL}), this involves an external mass being added to the body during the downward ('where this loading accentuates braking demand') action that is subsequently released at, or near the transition from downward to upward movement ('where the effect of accentuated eccentric loading enhances propulsion'). Research indicates that CMJ_{AEL} can acutely increase jump height by ~ 4.3 – 9.5% , peak power output by

CONTACT Thomas E. Bright  tommybright55@gmail.com  Youth Physical Development Centre, Cardiff School of Sport and Health Sciences, Cardiff Metropolitan University, Llandaff Campus, Western Avenue, Cardiff CF5 2YB, UK

© 2025 The Author(s). Published by Informa UK Limited, trading as Taylor & Francis Group.

This is an Open Access article distributed under the terms of the Creative Commons Attribution License (<http://creativecommons.org/licenses/by/4.0/>), which permits unrestricted use, distribution, and reproduction in any medium, provided the original work is properly cited. The terms on which this article has been published allow the posting of the Accepted Manuscript in a repository by the author(s) or with their consent.

~ 9.4–23.2% and peak vertical ground reaction force (vGRF) by ~ 3.9–6.3% (Aboodarda et al., 2013; Sheppard et al., 2007). In contrast, a recent study found improvements in braking but not propulsion during barbell and trap bar CMJ_{AEL} with fixed weight releaser loads at 10 kg, 20 kg and 30 kg (Taber et al., 2023). Differences in equipment, load selection, and participant characteristics across these studies may explain the conflicting results. Furthermore, there is currently limited information available on how CMJ_{AEL} could be applied to youth populations.

Regardless of the population, load or equipment used, there are methodological issues that must be addressed (Bright et al., 2024). First, the majority of studies that have investigated AEL during jumping movements have used force platforms to compute centre of mass (CoM) acceleration, velocity and displacement (Aboodarda et al., 2013; Harrison et al., 2019; Lloyd et al., 2022; Taber et al., 2023). While this provides valuable insight into CoM mechanics, the numerical integration process through which velocity and displacement are obtained is underpinned by the assumption that mass remains constant (Vanrenterghem et al., 2001). Specifically, bodyweight is usually calculated by averaging vGRF over 1 to 2 seconds before the jump starts and the participant is upright and motionless (Street et al., 2001). This is subsequently used to compute acceleration using Newton's second law of motion ($a = \sum(F - \text{bodyweight}) \div \text{bodymass}$) which is time-integrated once to derive CoM velocity, then again to calculate CoM displacement (Vanrenterghem et al., 2001). Given that the AEL mass is to be released shortly before or at the lowest position, the assumption of constant mass will be violated. For example, Aboodarda et al. (Aboodarda et al., 2013) reported peak concentric velocities of $0.36 \text{ m}\cdot\text{s}^{-1}$ and $0.42 \text{ m}\cdot\text{s}^{-1}$ alongside jump heights of 0.40 m and 0.42 m, respectively (measured as vertical displacement of the greater trochanter from quiet standing to apex of jump). However, based on the projectile motion equations and considering that peak concentric velocity occurs shortly before take-off (Cormie et al., 2009), these jump heights would require take-off velocities of approximately $2.80 \text{ m}\cdot\text{s}^{-1}$ and $2.87 \text{ m}\cdot\text{s}^{-1}$, respectively. This highlights a significant underestimation of velocity when the traditional method of forward integration (FI) is used during CMJ_{AEL}. With this information in mind, it is important that a more appropriate analysis is considered.

Bright et al. (Bright et al., 2024) recently published a method through which FI, as described above, is combined with backward integration (BI) to determine force-time characteristics during CMJ_{AEL}. This involves calculating CoM velocity and displacement using the initial

system mass (FI) and then again using body mass working backwards from the post-landing quiet standing period (BI). A previous study validated this method for calculating both maximal and submaximal unloaded CMJ height, though it depends on participants being instructed to quickly return to an upright and still position upon landing (Wade et al., 2022). In doing so, the combined FI:BI method enables accurate estimation of several CMJ_{AEL} variables, including jump height, reactive strength index modified (RSI_{mod}), countermovement depth, force at zero velocity and phase-specific time, vGRF and velocity (Bright et al., 2024). It is also important to note that this approach is considered appropriate here, as once the dumbbells are released, the movement is mechanically equivalent to an unloaded CMJ (Wade et al., 2022). While these are important findings, it is important that the methods are repeated in different samples and contexts to ensure the findings are generalisable to the population at large. Including agreement analysis is also essential, as statistical tests designed to detect differences (e.g., t-tests or ANOVA) are not suitable for determining whether measurement methods can be used interchangeably (McLaughlin, 2013).

The primary aim of the present study was to assess agreement and differences between CMJ_{AEL} variables obtained from force platform vGRF data using different numerical integration methods compared to a criterion. These included FI and BI, both on their own and combined (FI:BI; criterion), FI adjusted at the dumbbells release point (DR) and FI adjusted at the lowest position (BP) applied to CMJ_{AEL} with handheld dumbbells at 20% (CMJ_{AEL20}), 25% (CMJ_{AEL25}) and 30% (CMJ_{AEL30}) of body mass. The secondary aim was to assess the agreement between 3D motion capture (criterion) and vGRF in identifying the dumbbell release point. First, it was hypothesised that CMJ_{AEL} data calculated from the BI and DR integration methods would agree with the criterion FI:BI method, while the others would not. Second, it was hypothesised that the point of dumbbell release would agree between 3D motion capture and vGRF. Furthermore, it was hypothesised that the FI and BP integration methods would yield values significantly different from those produced by the FI:BI method across all conditions.

Material and methods

Experimental design

This study employed a within-participant repeated measures design with randomised counterbalancing to investigate agreement between numerical integration

techniques and methods of identifying the dumbbell release point during CMJ_{AEL}. Participants attended the biomechanics laboratory on two occasions, separated by approximately 72 hours: one for familiarisation and the second for data collection. There were three experimental conditions: CMJ_{AEL20}, CMJ_{AEL25} and CMJ_{AEL30}.

Participants

An a priori sample size estimation was performed using G*Power 3.1 software for a within-participant repeated-measures analysis of variance (ANOVA). The analysis assumed a medium effect size ($f = 0.25$), an alpha level of 0.05, and a desired statistical power of 0.80, yielding a minimum required sample size of 11 participants. Accordingly, 20 adolescent participants (10 males, 10 females; age: 15 ± 2 years; stature: 1.67 ± 0.10 m; body mass: 56.9 ± 12.2 kg; percentage of predicted adult height: 96.3 ± 2.6 %) volunteered for this study. All were free from injury and were involved in regular sport training and physical education-based activity programmes, inclusive of S&C a minimum of one time per week. Written parental consent, participant assent and completion of a standardised physical activity readiness questionnaire were obtained prior to participants being involved in the study. Ethical approval for the research was granted by the University Research Ethics Committee in accordance with the Declaration of Helsinki.

Maturity assessment

Standing height was collected using a stadiometer to the nearest 0.01 m (SECA 287, Vogel & Halke, Hamburg, Germany), and body mass was measured using digital scales to the nearest 0.1 kg (SECA mBCA 515, Vogel & Halke, Hamburg, Germany).

The biological maturity status of each participant was estimated using the Khamis-Roche percentage of predicted adult height method (Khamis & Roche, 1994). The associated mean error \pm standard deviation (SD) at the 50th percentile of this method was 2.2 ± 0.6 cm and 1.7 ± 0.6 cm between actual and predicted height in males and females aged between 4 and 17.5 years, respectively (Khamis & Roche, 1994). Participant's standing height, body mass, chronological age at observation and mid-parental standing height were used to apply this method (Khamis & Roche, 1994). Parental height was collected by a member of the research team, or where collection was not possible, it was self-reported by the parents and subsequently adjusted for overestimation (Epstein et al., 1995).

Percentage of predicted adult height was calculated by dividing participant's current height by their predicted adult height and multiplying this value by 100 (Khamis & Roche, 1994). Participants were allocated into three bands: pre-peak height velocity (PHV; <89%), circa-PHV (89–95%) and post-PHV (>95%), reflecting the somatic developmental stages of adolescence (Meylan et al., 2014; Molinari et al., 2013; Ruf et al., 2022). Six participants were classified as circa-peak height velocity (PHV) and 14 as post-PHV (Bright et al., 2023; Salter et al., 2022).

Testing procedures

Familiarisation

All participants were familiarised with the CMJ_{AEL} conditions, which involved beginning the movement in an upright position whilst keeping their body and both dumbbells motionless. Upon the command '3, 2, 1, jump!', participants were instructed to perform the countermovement at their maximum comfortable velocity, before releasing both dumbbells as close to the lowest position as possible without interrupting the movement fluidity to jump as high and as fast as possible (Bright et al., 2024). Participants were permitted a maximum of six practice trials to familiarise using CMJ_{AEL20} (mean \pm SD number of trials to familiarise = 5 ± 1). After releasing the dumbbells, participants were instructed to return their arms to an akimbo position for the remainder of the jump and landing.

Main data collection

A standardised 10-minute dynamic warm-up was completed before participants commenced each testing session. This began with 5 minutes of stationary cycling at a self-selected pace followed by 10 body weight squats, reverse lunges and jump squats. Participants then performed up to three CMJ_{AEL} trials increasing from 85% to 100% of perceived effort to refamiliarise with the movement. Following the warm-up, participants underwent three trials of each CMJ_{AEL} condition in a randomised order: a) CMJ_{AEL20} (a dumbbell of 10% of body mass in each hand); b) CMJ_{AEL25} (a dumbbell of 12.5% of body mass in each hand) and c) CMJ_{AEL30} (a dumbbell of 15% of body mass in each hand). Participants were provided with the following instruction before commencing each trial: '*perform the countermovement at your maximum comfortable speed, release the dumbbells as close to your lowest position as possible before moving upward and continue to jump as fast and as high as possible*'.

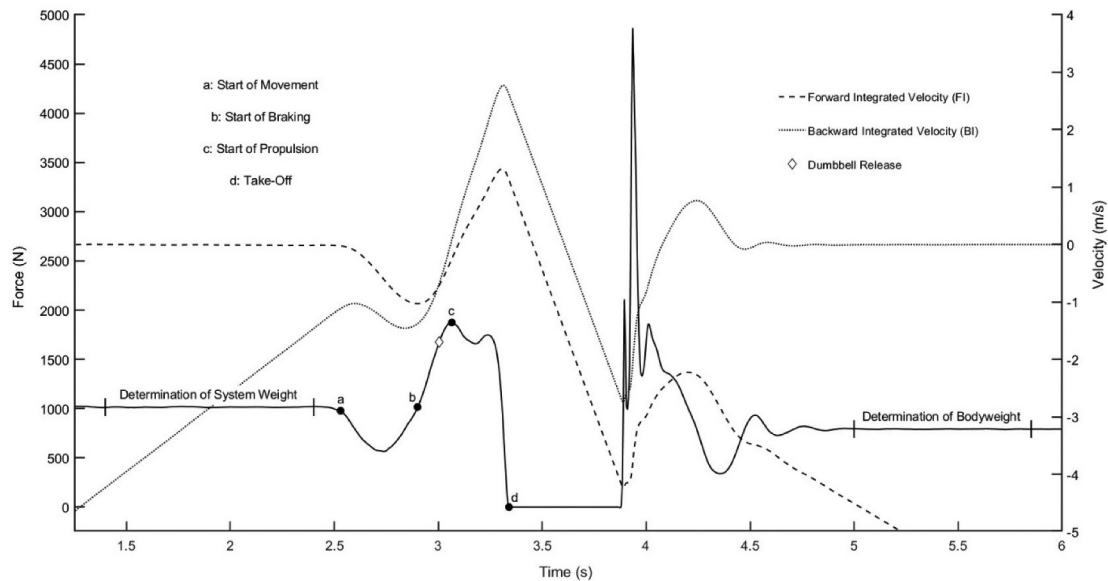


Figure 1. Force-time signal for a countermovement jump with accentuated eccentric loading (CMJ_{AEL}). Velocity-time signals, derived from forward integration (FI; dashed black line) and backward integration (BI; dotted black line), are also presented and the start of movement, dumbbell release, braking, propulsion and take-off points highlighted.

Equipment

Data from each trial were captured using two above ground parallel force platforms (Kistler Type 9286B, Kistler Instruments, Hampshire, United Kingdom) and a twelve-camera three-dimensional (3D) motion capture system (Miquis, Qualisys, Sweden) synchronously sampled at 1000 Hz and 250 Hz, respectively. Force platform and 3D motion capture systems were synchronised using a Kistler data acquisition board and a wired external trigger device. Forty-four spherical 14 mm retro-reflective markers were placed bilaterally over the following anatomical locations: sacrum, anterior iliac spine, posterior iliac spine, iliac crest, greater trochanter, lateral and medial epicondyle, lateral and medial malleolus, calcaneus, and first, second and fifth metatarsal head. Rigid four-marker cluster sets were placed on the lateral thighs and shanks to aid in thigh and shank segment tracking. The remaining three markers were secured on both ends and one of the sides of the right-hand dumbbell. Data were collected using Qualisys Track Manager software (Version 2023.3, Qualisys, Sweden).

Data analysis

Data were processed in Visual 3D biomechanical software (HAS-Motion, Inc., Germantown, MD). Raw vGRF signals from the two force platforms were summed to represent the vGRF acting at the whole-body CoM. The raw marker

trajectories were used to create a model that included pelvis and bilateral thigh, leg and foot segments and the right-hand dumbbell. Segment masses were assigned based on Dempster's regression equations (Dempster & Wilfrid, 1955), which estimate segment mass proportions relative to total body mass. The segments were modelled as cones and cylinders, following Hanavan's mathematical model for the human body (Hanavan, 1964). Hip joint centres were computed via regression from the anterior and posterior superior iliac spine markers (Bell et al., 1989) and knee and ankle joint centres were computed as the midpoint between the medial and lateral markers. The summed vGRF signal and marker trajectories were smoothed using a fourth-order, bidirectional, low-pass Butterworth digital filter with cut-off frequencies of 6 Hz and 50 Hz, respectively (Harry et al., 2022). The vGRF signal was filtered after time points of interest (described later) were located to ensure that it did not affect their location. The vGRF and dumbbell position data were processed to create time-histories for the following variables: summed vGRF, Model CoM, and dumbbell CoM, which were exported to MATLAB for further analysis (R2022b; The Mathworks, Inc., Natick, MA, USA) and down sampled to match the sampling frequency of the motion capture system (250 Hz).

Integration techniques

The integration techniques used in this study were similar to those recently employed (Figure 1) (Bright et al.,

2024). Briefly, the system weight was determined during a weighing period at the start (FI) or end (BI) of the jump to ensure an initial velocity of $0 \text{ m}\cdot\text{s}^{-1}$. The movement start was defined 30 ms prior to the first instance where the vGRF deviated from the mean by more than five times the SD (Owen et al., 2014), either exceeding the mean + 5*SD (pre-load strategy) or falling below the mean – 5*SD (unload strategy). Net vGRF was calculated by subtracting system weight from every timepoint, and CoM acceleration, velocity, and displacement were derived through numerical integration. The braking and propulsion phase start and endpoints were defined according to published guidelines (McMahon et al., 2018). Take-off and ground contact were defined using a 10 N threshold which was based on analysis of the residual vGRF signal when the force platforms were unloaded.

To facilitate comparisons with previous investigations (Aboodarda et al., 2013; Harrison et al., 2019; Taber et al., 2023), we also calculated the CoM velocity and displacement through manually adjusting system mass to body mass at the end of braking (BP) and dumbbell release point (DR). The dumbbell release point was identified using methods recently published (Bright et al., 2024). This involved examining the CoM and dumbbell acceleration signals to locate the first instance in which they differed by $\geq 2 \text{ m}\cdot\text{s}^{-2}$.

The following variables were extracted using all integration techniques: jump height, calculated as take-off velocity squared divided by 19.62 to estimate the vertical displacement of the CoM from take-off to the apex of the jump (Eythorsdottir et al., 2024); countermovement depth, defined as the change in CoM displacement between the start of movement and the end of the braking phase and the time duration, mean vGRF and velocity during braking and propulsion.

Statistical analyses

Agreement was examined using Bland-Altman repeated measures LOA alongside 95% confidence intervals (CI_{95}) for the mean bias and LOA (Bland & Altman, 2007; Hamilton & Stamey, 2007). A detailed guide and rationale for the repeated measures LOA analysis was recently reported (Wade et al., 2023). A two-way repeated measures ANOVA was used to examine differences in dependent variables across methods (FI:BI, FI, BI, BP, DR) and loads (CMJ_{AEL20} , CMJ_{AEL25} , CMJ_{AEL30}). Normality was assessed using the Shapiro–Wilk test and the absence of outliers was confirmed with boxplots. The Greenhouse–Geisser correction was used when the Mauchly’s sphericity test was violated and pairwise differences were identified using Bonferroni

post-hoc corrections. Effect sizes were calculated using Hedges’ *g* method, providing a measure of the magnitude of the differences in each variable noted between time points, and were interpreted as trivial (≤ 0.19), small (0.20 to 0.49), moderate (0.50 to 0.79) or large (≥ 0.80) (Cohen, 2009).

The two-way repeated measures and one-way ANOVA were performed in SPSS (IBM SPSS Statistics for Windows, Version 28.0; SPSS Inc., Chicago, IL, USA), and statistical significance was accepted at $p \leq 0.05$. All other analyses were undertaken in Microsoft Excel (version 2311, Microsoft Corp., Redmond, WA, USA).

Results

Differences

The two-way repeated measures ANOVA revealed significant interaction effects (‘method*load’) for all variables ($F \geq 5.567$; $p < 0.001$), with the exception of braking mean force ($F = 1.744$; $p = 0.093$). The main effect of ‘method’ was significant for the braking mean force ($F = 32.036$; $p < 0.001$); however, the main effect of ‘load’ was not significant ($F = 2.330$; $p = 0.111$). The pairwise comparisons and Hedge’s *g* effect size estimates are presented in Table 1.

Agreement

Tables 2–4 provide the mean bias, SD of bias, upper and lower 95% LOA, and CI_{95} for all methods and loading conditions. The BI and DR methods of calculating jump height agreed with the FI:BI method across all loading conditions. Jump height calculated using the FI and BP methods were less than FI:BI, with the differences increasing from CMJ_{AEL20} to CMJ_{AEL25} and CMJ_{AEL30} . Agreement between BI and FI:BI methods of calculating countermovement depth was good in all loading conditions. Although mean bias between DR and FI:BI methods was minimal, the LOA were relatively wide. Countermovement depth was greater in the DR method compared to FI:BI in the CMJ_{AEL25} condition.

The BI and DR methods of calculating braking and propulsion phase time agreed with the FI:BI method in all loading conditions. The FI and BP methods yielded different braking and propulsion phase times. Braking and propulsion mean force were similar between BI, DR, and FI:BI methods in all conditions. Braking mean force calculated using FI and BP methods were different from FI:BI in CMJ_{AEL20} and CMJ_{AEL30} and in CMJ_{AEL25} . Propulsion mean force calculated through FI and BP were different from FI:BI in CMJ_{AEL25} and CMJ_{AEL30} . Despite a difference observed between BI and FI:BI methods when calculating

Table 1. Descriptive statistics and Hedge's g effect size estimates with 95% confidence intervals for all loading conditions.

Variable	CMJ _{AEL20}			CMJ _{AEL25}			CMJ _{AEL30}			Hedges g (CI ₉₅)		
	Mean	SD		Mean	SD		Mean	SD		CMJ _{AEL20}	CMJ _{AEL25}	CMJ _{AEL30}
Jump Height (m)	FI:BI	0.263	0.042	0.262	0.042		0.262	0.037		6.06† (4.56, 7.55)	7.44† (5.66, 9.23)	8.96† (6.85, 11.06)
	FI	0.049	0.025	0.019	0.017		0.007	0.012		0.00 (-0.62, 0.62)	0.00 (-0.62, 0.62)	0.00 (-0.62, 0.62)
	BI	0.263	0.042	0.262	0.042		0.262	0.037		2.72† (1.85, 3.59)	4.31† (3.16, 5.46)	6.54† (4.94, 8.13)
Countermovement Depth (m)	BP	0.127	0.055	0.071	0.045		0.031	0.032		0.00 (-0.62, 0.62)	0.01 (-0.61, 0.63)	0.00 (-0.62, 0.62)
	DR	0.263	0.042	0.261	0.042		0.262	0.037		0.80* (0.16, 1.45)	1.08† (0.41, 1.74)	1.59† (0.87, 2.30)
	FI:BI	-0.314	0.058	-0.333	0.056		-0.319	0.062		0.00 (-0.62, 0.62)	0.00 (-0.62, 0.62)	0.00 (-0.62, 0.62)
Braking Phase Time (s)	FI	-0.374	0.085	-0.427	0.107		-0.472	0.119		0.80* (0.16, 1.45)	1.04† (0.38, 1.71)	1.53† (0.82, 2.23)
	BI	-0.314	0.058	-0.333	0.056		-0.319	0.062		-0.11 (-0.73, 0.51)	-0.48* (-1.11, 0.15)	-0.13 (-0.75, 0.49)
	BP	-0.374	0.085	-0.438	0.127		-0.488	0.141		-0.78† (-1.43, -0.14)	-0.51† (-1.14, 0.12)	-0.65† (-1.28, -0.01)
Propulsion Phase Time (s)	DR	-0.308	0.053	-0.308	0.047		-0.311	0.062		0.00 (-0.62, 0.62)	0.00 (-0.62, 0.62)	0.00 (-0.62, 0.62)
	FI:BI	0.231	0.115	0.334	0.235		0.442	0.273		0.00 (-0.62, 0.62)	0.00 (-0.62, 0.62)	0.00 (-0.62, 0.62)
	FI	0.339	0.154	0.471	0.285		0.627	0.289		1.85† (1.11, 2.60)	1.99† (1.23, 2.76)	2.61† (1.76, 3.46)
Braking Mean vGRF (N)	BI	0.231	0.115	0.334	0.235		0.442	0.273		0.00 (-0.62, 0.62)	0.00 (-0.62, 0.62)	0.00 (-0.62, 0.62)
	BP	0.339	0.154	0.494	0.299		0.662	0.303		0.00 (-0.62, 0.62)	0.00 (-0.62, 0.62)	0.00 (-0.62, 0.62)
	DR	0.231	0.115	0.334	0.235		0.442	0.273		0.00 (-0.62, 0.62)	0.00 (-0.62, 0.62)	0.00 (-0.62, 0.62)
Propulsion Mean vGRF (N)	FI:BI	0.329	0.054	0.338	0.054		0.338	0.057		0.00 (-0.62, 0.62)	0.00 (-0.62, 0.62)	0.00 (-0.62, 0.62)
	FI	0.222	0.059	0.202	0.077		0.155	0.079		1.85† (1.11, 2.60)	1.99† (1.23, 2.76)	2.61† (1.76, 3.46)
	BI	0.329	0.054	0.338	0.054		0.338	0.057		0.00 (-0.62, 0.62)	0.00 (-0.62, 0.62)	0.00 (-0.62, 0.62)
Braking Mean vGRF (N)	BP	0.222	0.059	0.180	0.063		0.120	0.039		1.85† (1.11, 2.60)	2.64† (1.78, 3.50)	4.37† (3.21, 5.54)
	DR	0.329	0.054	0.338	0.054		0.339	0.056		0.00 (-0.62, 0.62)	0.00 (-0.62, 0.62)	0.00 (-0.62, 0.62)
	FI:BI	887.2	199.2	872.7	242.1		829.4	194.8		-0.17† (-0.79, 0.45)	-0.18 (-0.80, 0.44)	-0.24* (-0.86, 0.38)
Propulsion Mean vGRF (N)	FI	922.8	208.3	917.8	245.3		877.1	197.1		0.00 (-0.62, 0.62)	0.00 (-0.62, 0.62)	0.00 (-0.62, 0.62)
	BI	887.2	199.2	872.7	242.1		829.4	194.8		0.00 (-0.62, 0.62)	0.00 (-0.62, 0.62)	0.00 (-0.62, 0.62)
	BP	922.8	208.3	918.3	245.5		878.0	197.3		-0.17† (-0.79, 0.45)	-0.18 (-0.80, 0.44)	-0.24* (-0.87, 0.38)
Braking Mean Velocity (m·s ⁻¹)	DR	887.4	199.5	872.7	242.1		829.2	194.7		0.00 (-0.62, 0.62)	0.00 (-0.62, 0.62)	0.00 (-0.62, 0.62)
	FI:BI	960.0	226.2	949.7	237.0		944.2	212.6		0.05 (-0.57, 0.67)	0.19* (-0.43, 0.81)	0.61† (-0.02, 1.25)
	FI	949.1	243.1	902.2	251.6		806.1	228.9		0.00 (-0.62, 0.62)	0.00 (-0.62, 0.62)	0.00 (-0.62, 0.62)
Propulsion Mean Velocity (m·s ⁻¹)	BI	960.0	226.2	949.7	237.0		944.2	212.6		0.00 (-0.62, 0.62)	0.00 (-0.62, 0.62)	0.00 (-0.62, 0.62)
	BP	949.1	243.1	906.3	251.9		813.7	227.5		0.05 (-0.57, 0.67)	0.17* (-0.45, 0.80)	0.58* (-0.05, 1.21)
	DR	960.0	226.0	949.7	237.0		944.3	212.6		0.00 (-0.62, 0.62)	0.00 (-0.62, 0.62)	0.00 (-0.62, 0.62)
Braking Mean Velocity (m·s ⁻¹)	FI:BI	-0.64	0.10	-0.61	0.15		-0.59	0.17		-0.08 (-0.70, 0.54)	0.33 (-0.29, 0.96)	0.37 (-0.25, 1.00)
	FI	-0.63	0.10	-0.66	0.17		-0.66	0.18		0.38 (-0.25, 1.01)	0.75 (0.11, 1.40)	1.36* (0.67, 2.05)
	BI	-0.68	0.09	-0.71	0.11		-0.83	0.17		0.25 (-0.38, 0.87)	0.27 (-0.35, 0.90)	0.27 (-0.35, 0.90)
Propulsion Mean Velocity (m·s ⁻¹)	BP	-0.63	0.10	-0.65	0.14		-0.64	0.15		0.00 (-0.62, 0.62)	-0.01 (-0.63, 0.61)	0.01 (-0.61, 0.63)
	DR	-0.64	0.10	-0.61	0.15		-0.60	0.17		4.67† (3.45, 5.89)	3.76† (2.71, 4.80)	4.27† (3.13, 5.42)
	FI:BI	1.30	0.09	1.29	0.11		1.28	0.10		0.00 (-0.62, 0.62)	0.00 (-0.62, 0.62)	0.00 (-0.62, 0.62)
Braking Mean Velocity (m·s ⁻¹)	FI	0.63	0.17	0.30	0.35		0.04	0.39		1.99† (1.22, 2.75)	3.09† (2.16, 4.02)	4.37† (3.21, 5.53)
	BI	1.30	0.09	1.29	0.11		1.28	0.10		0.00 (-0.62, 0.62)	0.00 (-0.62, 0.62)	0.00 (-0.62, 0.62)
	BP	0.96	0.22	0.74	0.22		0.49	0.23		0.00 (-0.62, 0.62)	0.00 (-0.62, 0.62)	0.00 (-0.62, 0.62)
Braking Mean Velocity (m·s ⁻¹)	DR	1.30	0.10	1.29	0.11		1.28	0.09		0.00 (-0.62, 0.62)	0.00 (-0.62, 0.62)	0.00 (-0.62, 0.62)

The effect size comparisons are calculated in reference to the FI:BI method. †significant difference ($p < 0.001$); *significant difference ($p < 0.05$); CI₉₅: 95% confidence intervals; SD: standard deviation.

Table 2. Repeated measures Bland-Altman for CMJ_{AEL20} force-time variables calculated using forward integration (FI), backward integration (BI), forward integration adjusted at the bottom position (BP) and at the dumbbell release point (DR), relative to combined forward:backward integration. The forward:backward integration signal represents the 'gold standard' method as it combines both processes to meet at the dumbbell release point.

Variable		Bias	Bias %	Bias CI ± 95	SD of Bias	LOA	Lower CI ± 95	Upper CI ± 95
Jump Height (m)	FI	0.209	81.49	0.206, 0.212	0.012	0.187, 0.232	0.178, 0.196	0.223, 0.241
	BI	0.000	0.00	0.000, 0.000	0.000	0.000, 0.000	0.000, 0.000	0.000, 0.000
	BP	0.132	51.67	0.127, 0.137	0.020	0.093, 0.171	0.078, 0.108	0.156, 0.187
	DR	0.000	0.00	0.000, 0.000	0.001	-0.001, 0.001	-0.002, -0.001	0.001, 0.002
Countermovement Depth (m)	FI	0.059	20.74	0.045, 0.073	0.053	-0.046, 0.163	-0.087, -0.004	0.122, 0.204
	BI	0.000	0.04	-0.001, 0.000	0.001	-0.003, 0.003	-0.004, -0.002	0.002, 0.004
	BP	0.059	20.74	0.045, 0.072	0.053	-0.046, 0.163	-0.087, -0.004	0.122, 0.204
	DR	-0.005	0.56	-0.017, 0.007	0.046	-0.095, 0.085	-0.131, -0.060	0.049, 0.121
Braking Phase Time (s)	FI	-0.106	50.38	-0.112, -0.099	0.025	-0.155, -0.057	-0.175, -0.136	-0.076, -0.037
	BI	0.000	0.00	0.000, 0.000	0.000	0.000, 0.000	0.000, 0.000	0.000, 0.000
	BP	-0.106	50.38	-0.112, -0.099	0.025	-0.155, -0.057	-0.175, -0.136	-0.076, -0.037
	DR	0.000	0.08	0.000, 0.000	0.001	-0.002, 0.002	-0.003, -0.001	0.001, 0.003
Propulsion Phase Time (s)	FI	0.106	29.96	0.099, 0.112	0.025	0.057, 0.155	0.037, 0.076	0.136, 0.175
	BI	0.000	0.00	0.000, 0.000	0.000	0.000, 0.000	0.000, 0.000	0.000, 0.000
	BP	0.106	29.96	0.099, 0.112	0.025	0.057, 0.155	0.037, 0.076	0.136, 0.175
	DR	0.000	0.00	0.000, 0.000	0.001	-0.002, 0.002	-0.003, -0.001	0.001, 0.003
Braking Mean vGRF (N)	FI	-32.58	3.63	-36.84, -28.32	16.49	-64.91, -0.25	-77.69, -52.12	-13.03, 12.53
	BI	0.00	0.00	0.00, 0.00	0.00	0.00, 0.00	0.00, 0.00	0.00, 0.00
	BP	-32.58	3.63	-36.84, -28.32	16.49	-64.91, -0.25	-77.69, -52.12	-13.03, 12.53
	DR	-0.29	0.03	-0.60, 0.02	1.20	-2.63, 2.05	-3.56, -1.71	1.13, 2.98
Propulsion Mean vGRF (N)	FI	13.12	1.66	7.38, 18.85	22.21	-30.41, 56.64	-47.61, -13.20	39.43, 73.84
	BI	0.00	0.00	0.00, 0.00	0.00	0.00, 0.00	0.00, 0.00	0.00, 0.00
	BP	13.12	1.66	7.38, 18.85	22.21	-30.41, 56.64	-47.61, -13.20	39.43, 73.84
	DR	0.10	0.00	-0.04, 0.24	0.54	-0.96, 1.15	-1.38, -0.54	0.74, 1.57
Braking Mean Velocity (m·s ⁻¹)	FI	-0.02	2.04	-0.03, -0.01	0.04	-0.10, 0.07	-0.13, -0.07	0.03, 0.10
	BI	0.03	6.44	0.01, 0.05	0.08	-0.12, 0.18	-0.18, -0.06	0.12, 0.24
	BP	-0.02	2.06	-0.03, -0.01	0.04	-0.10, 0.07	-0.13, -0.07	0.03, 0.10
	DR	0.00	0.07	0.00, 0.00	0.00	-0.01, 0.01	-0.01, -0.01	0.00, 0.01
Propulsion Mean Velocity (m·s ⁻¹)	FI	0.67	52.60	0.66, 0.69	0.05	0.57, 0.78	0.52, 0.61	0.74, 0.82
	BI	0.00	0.00	0.00, 0.00	0.00	0.00, 0.00	0.00, 0.00	0.00, 0.00
	BP	0.34	27.36	0.33, 0.36	0.07	0.22, 0.47	0.17, 0.27	0.42, 0.52
	DR	0.00	0.05	0.00, 0.00	0.00	-0.01, 0.01	-0.01, -0.01	0.00, 0.01

The agreement comparisons are calculated in reference to the FI:BI method. CI ± 95 : 95% confidence intervals; SD: standard deviation; LOA: limits of agreement.

braking mean velocity in CMJ_{AEL30}, there were no other meaningful differences between BI, DR, and FI:BI methods for braking and propulsion mean velocity across loading conditions. The FI and BP methods were not meaningfully different from FI:BI for braking mean velocity, despite wide LOA that increased with load. The FI and BP methods were different from FI:BI for propulsion mean velocity in CMJ_{AEL20}, CMJ_{AEL25} and CMJ_{AEL30}. The BI and DR methods were not different from FI:BI for propulsion mean velocity in any loading condition.

Time-normalised signals

A visual overview of the normalised velocity- and displacement-time signals and differences between signals is presented in Figures 2(a-f) and 3(a-f), respectively. The differences between FI:BI and FI and BP increased after the dumbbell release point. In contrast, the differences between FI:BI and BI were greater at the start of the movement and were near zero shortly after the dumbbell release point. There were no significant differences

detected between FI:BI and DR in any of the loading conditions. These observations highlight that the FI and BP methods tend to deviate more from the FI:BI method after the dumbbell release point, whereas the BI method shows greater differences at the start of the movement. The DR method demonstrated the strongest agreement with FI:BI for normalised velocity- and displacement-time signals in all loading conditions.

Dumbbell release identification

The repeated measures Bland-Altman plots (Figure 4 (a, c,e)) show the agreement between the 3D motion capture and vGRF methods for identifying the dumbbell release point. The mean bias are negative across all plots ($g = 0.18$ to 0.19 ; Bias % = -3.19 to -3.65), with LOA in CMJ_{AEL20}, CMJ_{AEL25}, and CMJ_{AEL30} being -0.17 to 0.02 s, -0.14 to -0.01 s, and -0.12 to -0.03 s, respectively. This indicates that the vGRF method tends to identify the dumbbell release point slightly later than the 3D motion capture method. The scatter of points

Table 3. Repeated measures Bland-Altman for CMJ_{AEL25} force-time variables calculated using forward integration (FI), backward integration (BI), forward integration adjusted at the bottom position (BP) and at the dumbbell release point (DR), relative to combined forward:backward integration. The forward:backward integration signal represents the 'gold standard' method as it combines both processes to meet at the dumbbell release point.

Variable		Bias	Bias (%)	CI ± 95	SD of Bias	LOA	Lower CI ± 95	Upper CI ± 95
Jump Height (m)	FI	0.238	92.81	0.235, 0.242	0.014	0.212, 0.265	0.201, 0.222	0.265, 0.288
	BI	0.000	0.00	0.000, 0.000	0.000	0.000, 0.000	0.000, 0.000	0.000, 0.000
	BP	0.187	72.35	0.183, 0.191	0.016	0.156, 0.218	0.143, 0.168	0.250, 0.283
	DR	0.000	0.02	0.000, 0.000	0.001	-0.001, 0.001	-0.002, -0.001	0.001, 0.002
Countermovement Depth (m)	FI	0.105	35.93	0.089, 0.122	0.064	-0.021, 0.232	-0.071, 0.029	0.228, 0.316
	BI	0.000	0.00	0.000, 0.000	0.000	0.000, 0.000	0.000, 0.000	0.000, 0.000
	BP	0.117	39.07	0.098, 0.137	0.075	-0.029, 0.264	-0.087, 0.029	0.253, 0.348
	DR	-0.015	0.46	-0.029, -0.001	0.054	0.092, -0.122	-0.164, -0.079	0.053, 0.121
Braking Phase Time (s)	FI	-0.137	55.55	-0.144, -0.130	0.026	-0.187, -0.087	-0.207, -0.167	-0.102, -0.003
	BI	0.000	0.00	0.000, 0.000	0.000	0.000, 0.000	0.000, 0.000	0.000, 0.000
	BP	-0.162	62.98	-0.171, -0.154	0.033	-0.227, -0.097	-0.253, -0.202	-0.170, -0.109
	DR	0.000	0.00	0.000, 0.000	0.000	0.000, 0.000	0.000, 0.000	0.002, 0.003
Propulsion Phase Time (s)	FI	0.137	39.92	0.130, 0.144	0.026	0.087, 0.187	0.067, 0.107	0.253, 0.352
	BI	0.000	0.00	0.000, 0.000	0.000	0.000, 0.000	0.000, 0.000	0.000, 0.000
	BP	0.162	45.46	0.154, 0.171	0.033	0.097, 0.227	0.072, 0.123	0.264, 0.325
	DR	0.000	0.00	0.000, 0.000	0.000	0.000, 0.000	0.000, 0.000	0.001, 0.002
Braking Mean vGRF (N)	FI	-42.59	5.16	-47.45, -37.74	18.79	-79.43, -5.76	-93.99, -64.86	-20.32, 8.80
	BI	0.00	0.00	0.00, 0.00	0.00	0.00, 0.00	0.00, 0.00	0.00, 0.00
	BP	-41.78	5.06	-47.59, -35.98	22.48	-85.84, 2.27	-103.26, -68.42	-15.15, 19.69
	DR	0.00	0.00	0.00, 0.00	0.00	0.00, 0.00	0.00, 0.00	0.00, 0.00
Propulsion Mean vGRF (N)	FI	50.22	5.68	44.85, 55.59	20.79	9.47, 90.97	-6.64, 25.58	74.86, 107.08
	BI	0.00	0.00	0.00, 0.00	0.00	0.00, 0.00	0.00, 0.00	0.00, 0.00
	BP	45.66	5.11	39.03, 52.30	25.68	-4.67, 96.00	-24.58, 15.23	76.09, 115.90
	DR	0.00	0.00	0.00, 0.00	0.00	0.00, 0.00	0.00, 0.00	0.00, 0.00
Braking Mean Velocity ($m \cdot s^{-1}$)	FI	0.05	9.85	0.03, 0.07	0.07	-0.09, 0.18	-0.14, -0.03	0.13, 0.24
	BI	0.09	24.42	0.06, 0.13	0.14	-0.19, 0.38	-0.30, -0.08	0.26, 0.49
	BP	0.03	6.90	0.01, 0.04	0.06	-0.10, 0.15	-0.14, -0.05	0.10, 0.20
	DR	0.00	0.03	0.00, 0.00	0.00	0.00, 0.00	-0.01, 0.00	0.00, 0.01
Propulsion Mean Velocity ($m \cdot s^{-1}$)	FI	0.99	78.85	0.96, 1.02	0.11	0.77, 1.20	0.69, 0.86	1.12, 1.29
	BI	0.00	0.00	0.00, 0.00	0.00	0.00, 0.00	0.00, 0.00	0.00, 0.00
	BP	0.55	43.11	0.53, 0.57	0.07	0.41, 0.69	0.35, 0.46	0.63, 0.74
	DR	0.00	0.02	0.00, 0.00	0.00	-0.01, 0.00	-0.01, 0.00	0.00, 0.01

The agreement comparisons are calculated in reference to the FI:BI method. CI ± 95 : 95% confidence intervals; SD: standard deviation; LOA: limits of agreement.

around the mean difference is consistent in the CMJ_{AEL20} and CMJ_{AEL25} conditions, suggesting constant difference between methods. However, CMJ_{AEL30} plot shows a trend of increasing negative differences with higher mean values, indicating a potential proportional bias.

The frequency distributions of the differences (Figure 4(b,d,f)) show a central tendency around $-0.1s$, corroborating the slight systematic bias where the vGRF method measures earlier than the 3D motion capture method. The spread of the differences ranges from approximately -0.25 to $0.05s$, with most values clustering near the central peak. The presence of a few outliers, particularly on the negative side, does not significantly affect the overall distributions.

Discussion

The primary aims of the present study were to assess agreement and differences between numerical integration methods compare to a criterion (FI, BI, BP and DR vs FI:BI) in calculating CMJ_{AEL} variables from force platform vGRF data. The secondary aim was to assess agreement between 3D motion capture and vGRF in identifying the

dumbbell release point. The first hypothesis was supported with agreement between numerical integration methods only acceptable for BI and DR methods. It was also hypothesised that 3D motion capture and vGRF methods would agree in identifying the dumbbell release point; however, the 3D motion capture method consistently identified the release prior to the vGRF method with wide LOA ($CMJ_{AEL20} = -0.17$ to 0.02 s; $CMJ_{AEL25} = -0.14$ to 0.01 s and $CMJ_{AEL30} = -0.12$ to 0.03 s). The final hypothesis was only partially supported, as most CMJ_{AEL} variables showed significant differences between FI and BP methods compared to the criterion FI:BI method.

Our results are in agreement with recent findings (Bright et al., 2024) and demonstrate that only BI and DR integration methods can be used to accurately calculate jump height, countermovement depth and braking and propulsion phase time, mean vGRF and mean velocity from force platform data. At present, however, the body of literature investigating the performance enhancing effects of AEL applied to vertical jumping tasks have utilised FI or BP methods (Aboodarda et al., 2013; Harrison et al., 2019; Lloyd

Table 4. Repeated measures Bland-Altman for CMJ_{AEL30} force-time variables calculated using forward integration (FI), backward integration (BI), forward integration adjusted at the bottom position (BP) and at the dumbbell release point (DR), relative to combined forward:backward integration. The forward:backward integration signal represents the 'gold standard' method as it combines both processes to meet at the dumbbell release point.

Variable		Bias	Bias (%)	CI ± 95	SD of Bias	LOA	Lower CI ± 95	Upper CI ± 95
Jump Height (m)	FI	0.248	97.33	0.244, 0.252	0.015	0.220, 0.277	0.208, 0.231	0.265, 0.288
	BI	0.000	0.00	0.000, 0.000	0.000	0.000, 0.000	0.000, 0.000	0.000, 0.000
	BP	0.225	88.15	0.220, 0.231	0.021	0.184, 0.267	0.168, 0.200	0.250, 0.283
	DR	0.000	0.00	0.000, 0.000	0.001	0.001, -0.001	-0.002, -0.001	0.001, 0.002
Countermovement Depth (m)	FI	0.160	54.56	0.145, 0.175	0.057	0.048, 0.272	0.004, 0.093	0.228, 0.316
	BI	0.000	0.00	0.000, 0.000	0.000	0.000, 0.000	0.000, 0.000	0.000, 0.000
	BP	0.179	60.44	0.163, 0.195	0.062	0.058, 0.300	0.011, 0.106	0.253, 0.348
	DR	0.000	2.18	-0.011, 0.012	0.044	-0.086, 0.087	-0.120, -0.052	0.053, 0.121
Braking Phase Time (s)	FI	-0.177	66.84	-0.194, -0.161	0.064	-0.302, -0.052	-0.352, -0.253	-0.102, -0.003
	BI	0.000	0.00	0.000, 0.000	0.000	0.000, 0.000	0.000, 0.000	0.000, 0.000
	BP	-0.217	76.48	-0.227, -0.207	0.040	-0.295, -0.140	-0.325, -0.264	-0.170, -0.109
	DR	0.000	0.15	0.000, 0.001	0.001	-0.002, 0.002	-0.002, -0.001	0.002, 0.003
Propulsion Phase Time (s)	FI	0.177	52.96	0.161, 0.194	0.064	0.052, 0.302	0.003, 0.102	0.253, 0.352
	BI	0.000	0.00	0.000, 0.000	0.000	0.000, 0.000	0.000, 0.000	0.000, 0.000
	BP	0.217	62.57	0.207, 0.227	0.040	0.140, 0.295	0.109, 0.170	0.264, 0.325
	DR	0.000	0.10	-0.001, 0.000	0.001	-0.002, 0.002	-0.003, -0.002	0.001, 0.002
Braking Mean vGRF (N)	FI	-42.66	5.51	-50.00, -35.32	28.40	-98.33, 13.01	-120.34, -76.32	-9.00, 35.02
	BI	0.00	0.00	0.00, 0.00	0.00	0.00, 0.00	0.00, 0.00	0.00, 0.00
	BP	-44.13	5.73	-51.55, -36.72	28.70	-100.39, 12.12	-122.63, -78.15	-10.12, 34.36
	DR	0.17	0.02	-0.03, 0.37	0.79	-1.38, 1.72	-1.99, -0.76	1.11, 2.33
Propulsion Mean vGRF (N)	FI	130.82	13.87	106.43, 155.21	94.40	-54.21, 315.85	-127.37, 18.95	242.69, 389.01
	BI	0.00	0.00	0.00, 0.00	0.00	0.00, 0.00	0.00, 0.00	0.00, 0.00
	BP	122.81	12.84	95.42, 150.20	106.04	-85.03, 330.65	-167.21, -2.85	248.47, 412.83
	DR	-0.04	0.01	-0.19, 0.11	0.58	-1.18, 1.10	-1.63, -0.73	0.65, 1.55
Braking Mean Velocity (m·s ⁻¹)	FI	0.07	14.42	0.05, 0.09	0.09	0.09, 0.24	-0.16, -0.03	0.17, 0.30
	BI	0.21	52.40	0.15, 0.26	0.21	-0.21, 0.62	-0.37, -0.04	0.46, 0.78
	BP	0.04	10.68	0.03, 0.06	0.05	-0.05, 0.14	-0.09, -0.01	0.10, 0.18
	DR	0.00	0.17	0.00, 0.00	0.00	0.00, 0.01	-0.01, 0.00	0.01, 0.01
Propulsion Mean Velocity (m·s ⁻¹)	FI	1.25	100.10	1.22, 1.28	0.13	1.00, 1.50	0.90, 1.10	1.40, 1.60
	BI	0.00	0.00	0.00, 0.00	0.00	0.00, 0.00	0.00, 0.00	0.00, 0.00
	BP	0.77	60.13	0.72, 0.82	0.19	0.39, 1.14	0.24, 0.54	1.00, 1.29
	DR	0.00	0.09	0.00, 0.00	0.00	-0.01, 0.01	-0.01, 0.00	0.01, 0.01

The agreement comparisons are calculated in reference to the FI:BI method. CI ± 95 : 95% confidence intervals; SD: standard deviation; LOA: limits of agreement.

et al., 2022; Taber et al., 2023). In doing so, an accurate estimate of body mass from a stationary standing period is required to compute CoM acceleration through Newton's second law of motion, which is then integrated once to obtain CoM velocity and twice for CoM displacement. The problem arises from the release of dumbbells resulting in a change of mass from the release location to takeoff. Following FI does not account for this change in mass and therefore results in the largest error. The BP method has been used in previous studies in an attempt to account for the change in mass (Harrison et al., 2019); however, the results of the current study suggest that this method amends the mass at the incorrect timepoint, compromising the accuracy of subsequent calculations during propulsion and landing. It assumes that the dumbbells are released precisely at the participant's lowest position, which was not supported in the current study. The FI:BI and DR methods overcome this shortcoming and account for the change in mass at the correct timepoint. However, it is important to note that participants must return to an upright still position as quickly as possible upon landing to ensure that the

estimation of body mass and integration is accurate (Burnett et al., 2023; Street et al., 2001; Wade et al., 2022).

The current findings suggest that previous studies in which only vGRF data has been considered in analysing jumps with AEL should be interpreted with caution (Bright et al., 2024). For example, Harrison et al. (Harrison et al., 2019) found 15 kg dumbbells disrupted the relative timing and coordination of the CMJ_{AEL} owing to moderate to large increases in countermovement ('eccentric') duration and significant reductions in propulsion time when compared to bodyweight and weighted vest CMJs with 15 kg. However, the authors of this study manually adjusted the calculation of CoM velocity at the point at which 0 m·s⁻¹ velocity was identified and assumed that this reflected the dumbbell release location (BP method). We found that this approach delayed the point at which CoM velocity reached 0 m·s⁻¹ because the change in mass resulting from the dumbbell release caused a significant difference in the CoM velocity data (Bright et al., 2024). Subsequently, this leads to an overestimation of the unweighting and braking duration and an

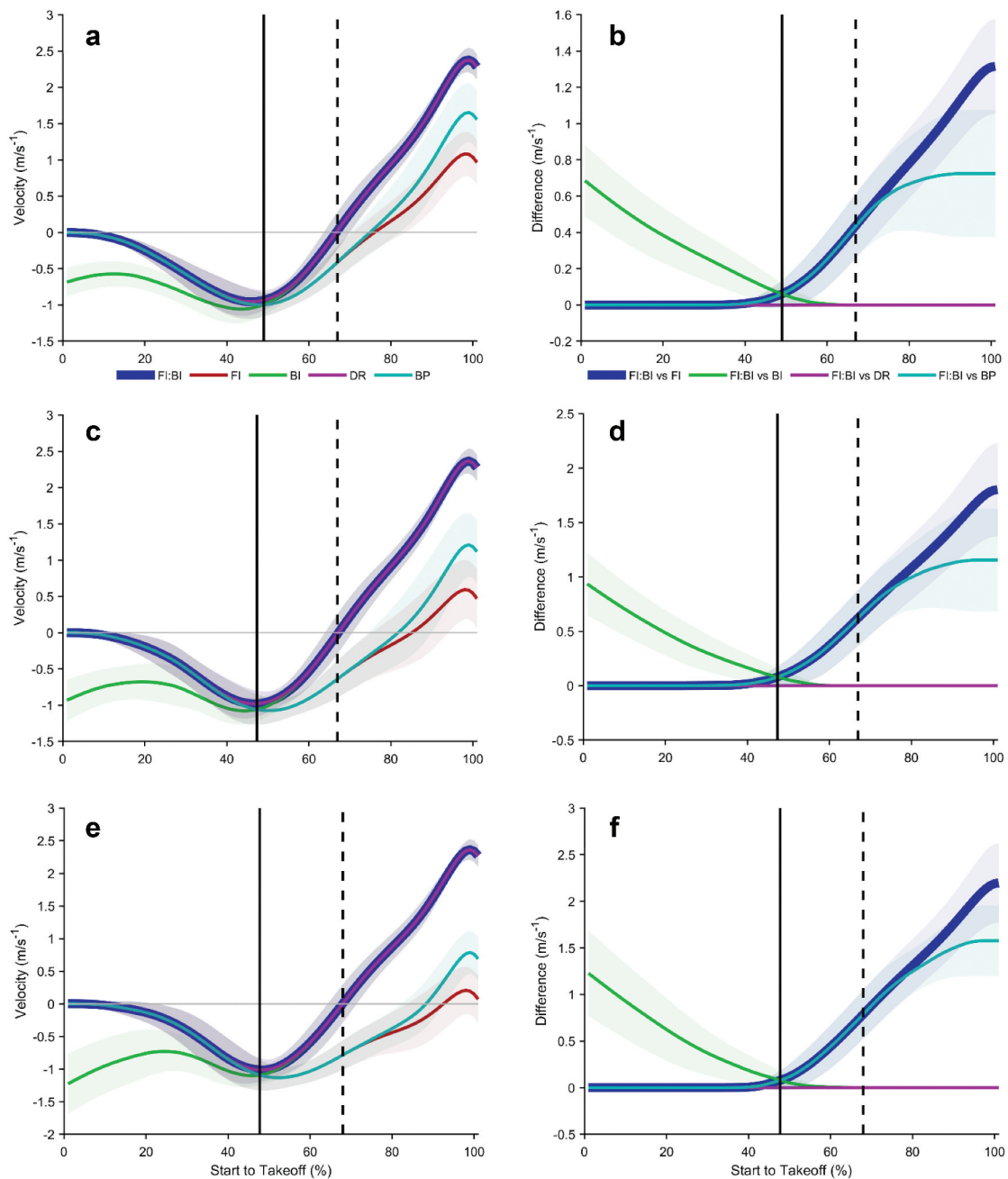


Figure 2. Normalised velocity-time signals for forward:backward integration (FI:BI), forward integration (FI), backward integration (BI), forward integration adjusted at dumbbell release (DR) and forward integration adjusted at bottom position (BP), alongside differences. Mean and SD velocity-time signals and respective differences for CMJ_{AEL20} , CMJ_{AEL25} and CMJ_{AEL30} are presented in figures a and b, c and d, and e and f, respectively. In each figure, the solid vertical line represents the dumbbell release point and the dashed vertical line represents the bottom position.

underestimation of the propulsive duration. A more recent study reported negligible-small reductions in jump height during barbell and trap bar CMJ_{AEL} with fixed eccentric loads using weight releasers at 10 kg, 20 kg and 30 kg (Taber et al., 2023). The authors concluded that this was likely due to an overall decrease in propulsive phase performance, despite an increase in braking force. Interestingly, the same authors omitted

countermovement depth, velocity and power from their analysis because of its poor reliability (Taber et al., 2023). However, this poor reliability may be better explained by the change in mass not being accounted for during integration. Indeed, countermovement depth recorded the poorest reliability of all variables, which is logical when considering that it is calculated via double integration (Bright et al., 2024). Together, these findings

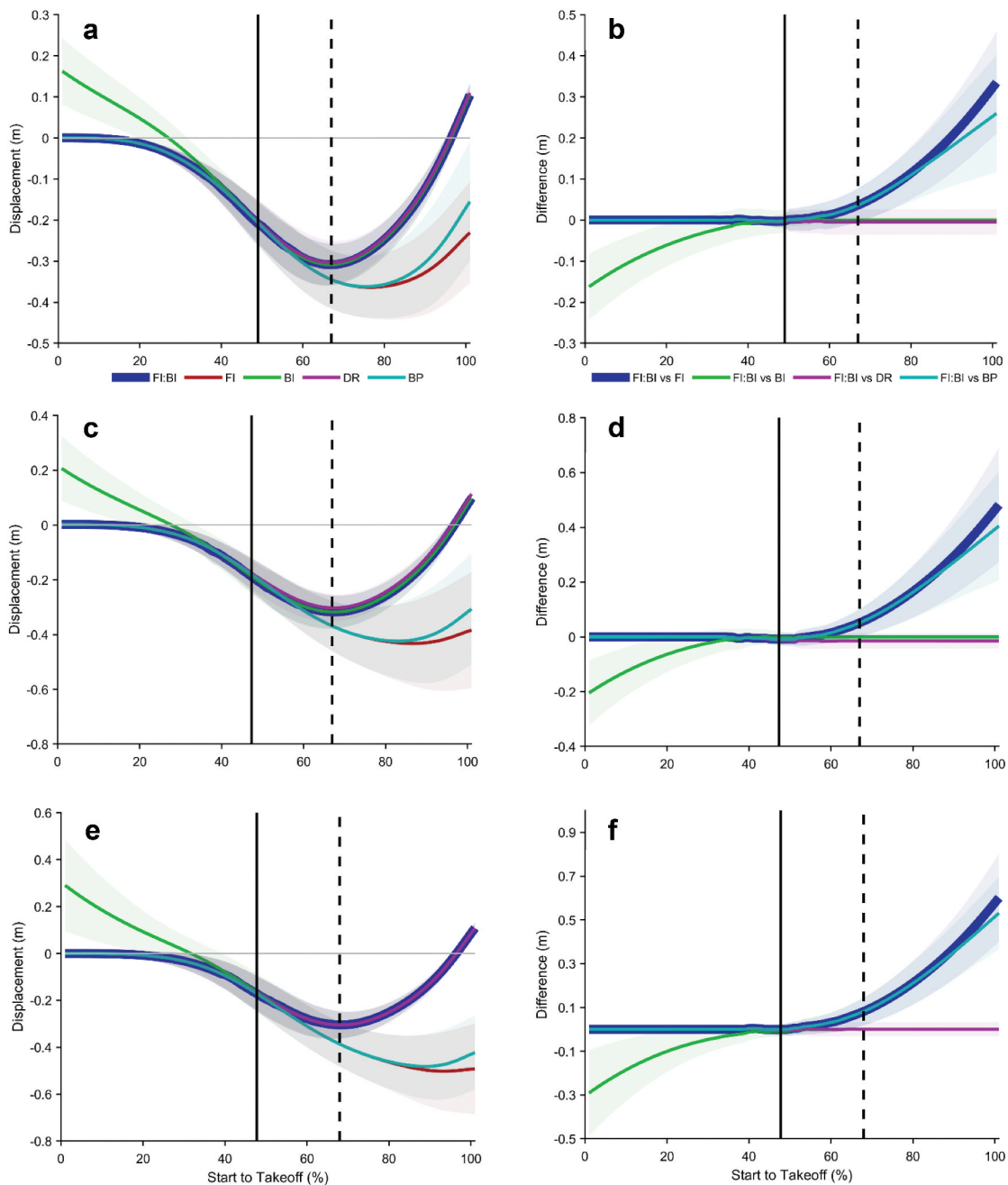


Figure 3. Normalised displacement-time signals for forward:backward integration (FI:BI), forward integration (FI), backward integration (BI), forward integration adjusted at dumbbell release (DR) and forward integration adjusted at bottom position (BP), alongside differences. Mean and SD displacement-time signals and respective differences for CMJ_{AEL20} , CMJ_{AEL25} and CMJ_{AEL30} are presented in figures a and b, c and d, and e and f, respectively. In each figure, the solid vertical line represents the dumbbell release point and the dashed vertical line represents the bottom position.

highlight the necessity for accurate identification and integration of mass changes during CMJ_{AEL} , as a failure to do so can lead to erroneous conclusions.

Research into the performance-enhancing effects of AEL in youth populations is limited to one study where the drop jump was used (Lloyd et al., 2022). Although the authors reported an increase in ground contact time and subsequent reductions in spring-like

behaviour, it is important to note that there were meaningful increases in jump height alongside braking and propulsive impulse. These findings suggest that further research in this area is warranted, particularly through the incorporation of a technically easier movement to execute in the CMJ (Gillen et al., 2019). Furthermore, investigation into the benefits of AEL during drop jumps could be revisited after a period

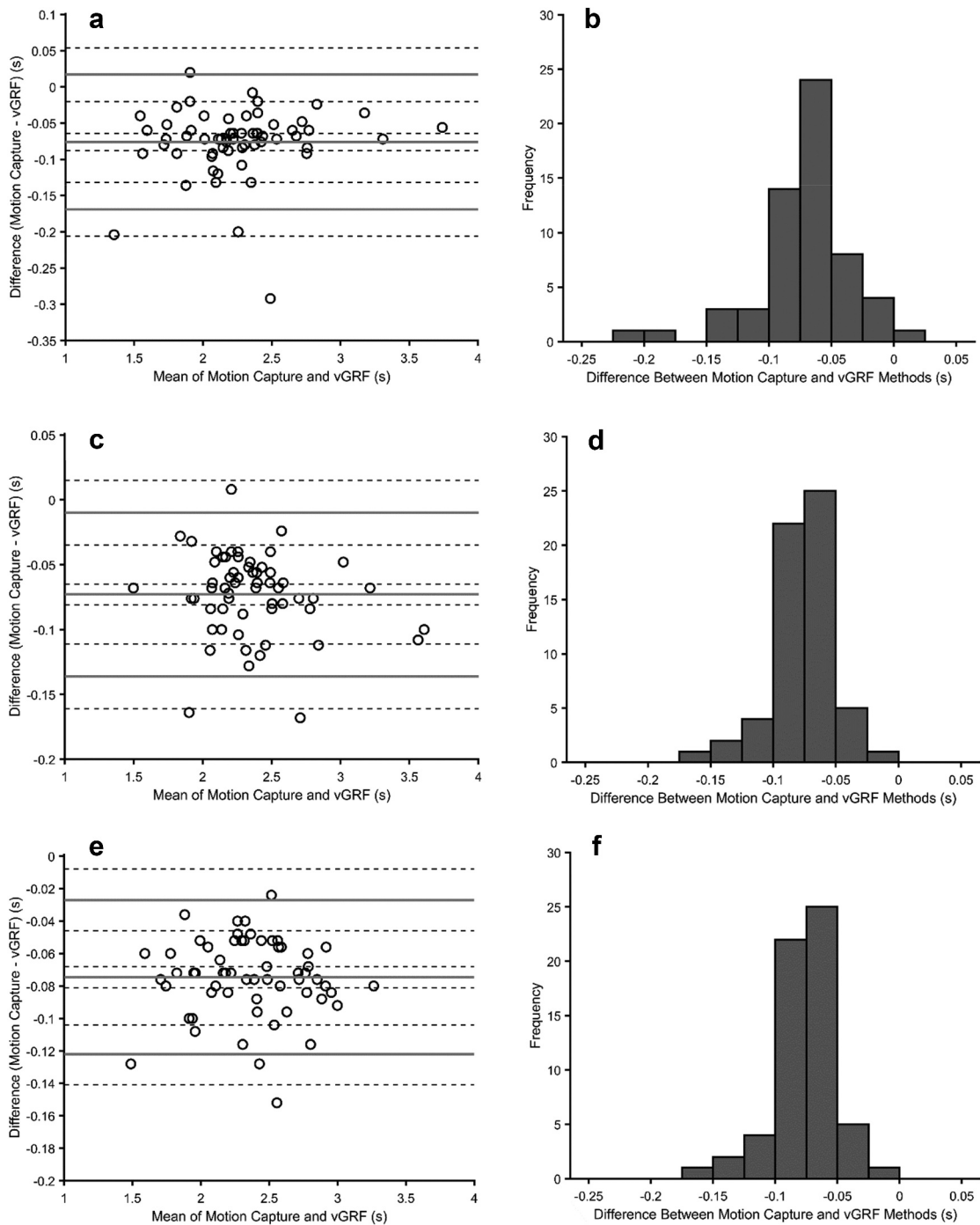


Figure 4. Repeated measures Bland-Altman assessment of agreement between motion capture and vGRF methods to locate the dumbbell release point. Note: figures a, c and e illustrate the Bland-Altman plots for each of the CMJ_{AEL20} , CMJ_{AEL25} and CMJ_{AEL30} conditions, while figures b, d, and f illustrate the frequency distribution for the differences between the methods for each of the CMJ_{AEL20} , CMJ_{AEL25} and CMJ_{AEL30} conditions. The solid grey lines represent the bias and upper and lower limits of agreement, and the dashed black lines represent the 95% confidence intervals for the bias and upper and lower limits of agreement.

of dedicated CMJ_{AEL} training. Given the widespread use of force platforms in research and S&C practice, the findings of this study are particularly important as they highlight methodological issues that significantly impact data accuracy and subsequently any CMJ_{AEL} training-related decisions that these data may be

used for. Specifically, as the ability to utilise the SSC in movements such as the CMJ can be augmented with relevant training methods (Asadi et al., 2018; Ramirez-Campillo et al., 2023), it is important that CMJ_{AEL} is accurately captured and not confounded by methodological inaccuracies.

The second aim of this study was to compare 3D motion capture and vGRF methods in identifying the dumbbell release point during CMJ_{AEL}. The Bland-Altman plots in Figure 4 demonstrate a negative mean bias in all loading conditions. The LOA indicates some variability between methods; however, a deeper inspection of the data reveals a different perspective. In agreement with recent findings (Bright et al., 2024), the 3D motion capture method appears to locate the initiation of the release (i.e., the hand begins to open and the dumbbells' acceleration reduces in preparation for release). In contrast, the vGRF method identifies the point at which the dumbbell release is completed, as indicated by the momentary interaction of the FI (system mass) and BI (body mass) signals before they transition to assume each other's magnitude. Therefore, the variability observed in the LOA may represent the duration over which the release takes place (i.e., time between initiation and release). To keep with the assumptions underpinning numerical integration (Burnett et al., 2023; Kibele, 1998; Street et al., 2001), we recommend that the vGRF method is used to identify the dumbbell release when using force platforms. The rationale for this is clearly illustrated in Figures 2 and 3 whereby the DR method demonstrates accurate velocity and displacement calculations post dumbbell release. If this was not the case, the DR velocity- and displacement-time signals would not agree with the criterion (i.e., FI:BI). Although the observed bias is relatively small, its practical relevance depends on the level of temporal precision required in the analysis of CMJ_{AEL}. For example, if an S&C practitioner is interested in phase-specific variables, the accurate identification of the dumbbell release timing becomes more critical. In this situation, ensuring that participants are upright and motionless at the start and end of a CMJ_{AEL} is essential to maintain analytical accuracy. Conversely, if the primary outcome is limited to jump height, the exact timing of dumbbell release may be of less consequence; however, this should be taken into account in future research.

While the results of this study provide valuable insights into the challenges of analysing vGRF from CMJ_{AEL} in youth athletes, it is not without its limitations. First, the dumbbell release point identified using 3D motion capture was done so via analysis of the CoM and dumbbell segment acceleration data. It is possible that more accurate information could be gathered if markers were placed on the dumbbell and hand; however, this approach was difficult to follow given our experimental set up and sample population. Future research should consider using a comprehensive whole-body 3D marker set to enable more accurate estimation of CoM and facilitate direct comparisons with the FI:BI

criterion used in the present study. The sample size and specificity of the youth athlete population studied limit the generalisability of the results, as different populations or larger groups might exhibit varying responses to CMJ_{AEL}. Although the biological maturity status was calculated, it was not formally included in the analysis. It is possible that more mature participants (i.e., post-PHV), who may have greater levels of muscular strength and coordination, responded differently to CMJ_{AEL}. Furthermore, we did not conduct a sex-specific analysis; male and female participants were grouped together, which may have obscured potential differences between sexes. While these are valid limitations, it is important to note that the primary aim of this study was to investigate analytical approaches for processing vGRF data during CMJ_{AEL}, rather than to evaluate performance differences or responses to the loading conditions themselves. Finally, previous work has also explored the use of alternative equipment (i.e., barbells and trap bars) and VJ exercises (i.e., DJ). Future studies should therefore investigate a variety of exercises and equipment to truly understand the utility of AEL during vertical tasks.

Conclusion and practical applications

The present investigation provides clear guidelines for accurately collecting and analysing force platform vGRF during CMJ_{AEL} in youth athletes. Our findings demonstrate that a combination of FI and BI techniques yields the most accurate calculations of key performance variables during CMJ_{AEL} because it accounts for the release of dumbbells. We also display the agreement between 3D motion capture and force platform vGRF methods in identifying the dumbbell release. Given that the vGRF method consistently identified the dumbbell release in delay of the criterion method (i.e., 3D motion capture), these methods should not be used interchangeably. However, we believe that the 3D motion capture method is better suited to locate the initiation of the release, whereas the vGRF method locates separation of the dumbbell from the participant's hands, as evidenced by the accuracy of the DR method in calculating CoM velocity and displacement post release. Therefore, it appears that the vGRF method is suitable to locate the point of dumbbell release when researchers or practitioners only have access to force platforms. Overall, this investigation provides important information regarding the analyses of CMJ_{AEL} that should be adopted in future research and practice.

Disclosure statement

Dr. Peter Mundy is the Chief Scientific Officer and Professor Jason Lake is the Director of Education at Hawkin Dynamics Inc.

Funding

The author(s) reported that there is no funding associated with the work featured in this article.

ORCID

Thomas E. Bright  <http://orcid.org/0000-0001-8089-817X>

References

- Aboodarda, S. J., Yusof, A., Osman, N. A. A., Thompson, M. W., & Mokhtar, A. H. (2013). Enhanced performance with elastic resistance during the eccentric phase of a countermovement jump. *International Journal of Sports Physiology and Performance*, 8(2), 181–187. <https://doi.org/10.1123/ijpspp.8.2.181>
- Asadi, A., Ramirez-Campillo, R., Arazi, H., & Sáez de Villarreal, E. (2018). The effects of maturation on jumping ability and sprint adaptations to plyometric training in youth soccer players. *Journal of Sports Sciences*, 36(21), 2405–2411. <https://doi.org/10.1080/02640414.2018.1459151>
- Bell, A. L., Brand, R. A., & Pedersen, D. R. (1989). Prediction of hip joint centre location from external landmarks. *Human Movement Science*, 8(1), 3–16. [https://doi.org/10.1016/0167-9457\(89\)90020-1](https://doi.org/10.1016/0167-9457(89)90020-1)
- Bland, J. M., & Altman, D. G. (2007). Agreement between methods of measurement with multiple observations per individual. *Journal of Biopharmaceutical Statistics*, 17(4), 571–582. <https://doi.org/10.1080/10543400701329422>
- Bright, T., Handford, M. J., Hughes, J. D., Mundy, P. D., Lake, J. P., & Daggart, L. (2023). Development and reliability of countermovement jump performance in youth athletes at pre-, circa- and post-peak height velocity: Countermovement jump reliability in youth athletes. *International Journal of Strength and Conditioning*, 3(1). <https://journal.iusca.org/index.php/Journal/article/view/149>
- Bright, T. E., Harry, J. R., Lake, J., Mundy, P., Theis, N., & Hughes, J. D. (2024). Methodological considerations in assessing countermovement jumps with handheld accentuated eccentric loading. *Sports Biomechanics*, 0, 1–18. <https://doi.org/10.1080/14763141.2024.2374884>
- Burnett, J. K., Kim, Y.-W., Kwon, H. J., Miller, R. H., & Shim, J. K. (2023). Whole body mass estimates and error propagation in countermovement jump: A simulated error study. *Sports Biomechanics*, 1–14. <https://doi.org/10.1080/14763141.2023.2236589>
- Cohen, J. (2009). *Statistical power analysis for the behavioral sciences* (2. ed. reprint ed.). Psychology Press.
- Cormie, P., McBride, J. M., & McCaulley, G. O. (2009). Power-time, Force-time, and velocity-time curve analysis of the countermovement jump: Impact of training. *The Journal of Strength & Conditioning Research*, 23(1), 177. <https://doi.org/10.1519/JSC.0b013e3181889324>
- Dantas, M., de Queiros, V. S., de Fonseca, F. S., Almeida-Neto, P. F. D., Teixeira, R. V., Silva, L. M. D., Aidar, F. J., Matos, D. G. D., & Cabral, B. G. D. A. T. (2020). The stretch-shortening cycle efficiency is dependent on the maturational stage. *Revista Brasileira de Cineantropometria & Desempenho Humano*, 22, e72597. <https://doi.org/10.1590/1980-0037.2020v22e72597>
- Dempster, W. T. (Wilfrid, T. (1955. *Space requirements of the seated operator: Geometrical, kinematic, and Mechanical aspects of the body, with special reference to the limbs.* <http://deepblue.lib.umich.edu/handle/2027.42/4540>
- Epstein, L. H., Valoski, A. M., Kalarchian, M. A., & McCurley, J. (1995). Do children lose and maintain weight easier than adults: A comparison of child and parent weight changes from six months to Ten years. *Obesity Research*, 3(5), 411–417. <https://doi.org/10.1002/j.1550-8528.1995.tb00170.x>
- Eythorsdottir, I., Gløersen, Ø., Rice, H., Werkhausen, A., Ettema, G., Mentzoni, F., Solberg, P., Lindberg, K., & Paulsen, G. (2024). The battle of the equations: A systematic review of jump height calculations using force platforms. *Sports Medicine*, 54(11), 2771–2791. <https://doi.org/10.1007/s40279-024-02098-x>
- Gillen, Z. M., Jahn, L. E., Shoemaker, M. E., McKay, B. D., Mendez, A. I., Bohannon, N. A., & Cramer, J. T. (2019). Effects of eccentric preloading on concentric vertical jump performance in youth athletes. *Journal of Applied Biomechanics*, 35(5), 327–335. <https://journals.humankinetics.com/view/journals/jab/35/5/article-p327.xml>
- Gillen, Z. M., Shoemaker, M. E., McKay, B. D., Bohannon, N. A., Gibson, S. M., & Cramer, J. T. (2022). Influences of the stretch-shortening cycle and arm swing on vertical jump performance in children and adolescents. *The Journal of Strength & Conditioning Research*, 36(5), 1245. <https://doi.org/10.1519/JSC.0000000000003647>
- Hamilton, C., & Stamey, J. (2007). Using Bland–Altman to assess agreement between two Medical devices - Don't forget the confidence intervals! *Journal of Clinical Monitoring and Computing*, 21(6), 331–333. <https://doi.org/10.1007/s10877-007-9092-x>
- Hanavan, E. P. (1964). *A mathematical model of the human body.* Aerospace Medical Research Laboratories, Aerospace Medical Division, Air Force Systems Command.
- Harrison, A. J., Byrne, P., & Sundar, S. (2019). The effects of added mass on the biomechanics and performance of countermovement jumps. *Journal of Sports Sciences*, 37(14), 1591–1599. <https://doi.org/10.1080/02640414.2019.1577120>
- Harry, J. R., Blinch, J., Barker, L. A., Krzyzskowski, J., & Chowning, L. (2022). Low-Pass filter effects on metrics of countermovement vertical jump performance. *Journal of Strength and Conditioning Research*, 36(5), 1459–1467. <https://doi.org/10.1519/JSC.0000000000003611>
- Khamis, H. J., & Roche, A. F. (1994). Predicting adult stature without using skeletal age: The khamis-Roche method. *Pediatrics*, 94(4), 504–507. <https://doi.org/10.1542/peds.94.4.504>
- Kibele, A. (1998). Possibilities and limitations in the biomechanical analysis of countermovement jumps: A methodological study. *Journal of Applied Biomechanics*, 14(1), 105–117. <https://doi.org/10.1123/jab.14.1.105>
- Lloyd, R. S., Howard, S. W., Pedley, J. S., Read, P. J., Gould, Z. I., & Oliver, J. L. (2022). The acute effects of accentuated eccentric loading on drop jump kinetics in adolescent athletes. *Journal of Strength and Conditioning Research*, 36(9), 2381–2386. <https://doi.org/10.1519/JSC.0000000000003911>
- Malisoux, L., Francaux, M., Nielens, H., & Theisen, D. (2006). Stretch-shortening cycle exercises: An effective training paradigm to enhance power output of human single muscle fibers. *Journal of Applied Physiology*, 100(3), 771–779. <https://doi.org/10.1152/jappphysiol.01027.2005>

- McLaughlin, P. (2013). Testing agreement between a new method and the gold standard-how do we test? *Journal of Biomechanics*, 46(16), 2757–2760. <https://doi.org/10.1016/j.jbiomech.2013.08.015>
- McMahon, J. J., Suchomel, T. J., Lake, J. P., & Comfort, P. (2018). Understanding the key phases of the countermovement jump force-time curve. *Strength & Conditioning Journal*, 40(4), 96. <https://doi.org/10.1519/SSC.0000000000000375>
- Meylan, C. M. P., Cronin, J., Oliver, J. L., Hopkins, W. G., & Pinder, S. (2014). Contribution of vertical Strength and power to sprint performance in young male athletes. *International Journal of Sports Medicine*, 35(9), 749–754. <https://doi.org/10.1055/s-0033-1363191>
- Molinari, L., Gasser, T., & Largo, R. (2013). A comparison of skeletal maturity and growth. *Annals of Human Biology*, 40(4), 333–340. <https://doi.org/10.3109/03014460.2012.756122>
- Owen, N. J., Watkins, J., Kilduff, L. P., Bevan, H. R., & Bennett, M. A. (2014). Development of a criterion method to determine peak mechanical power output in a countermovement jump. *The Journal of Strength & Conditioning Research*, 28(6), 1552. <https://doi.org/10.1519/JSC.0000000000000311>
- Pedley, J. S., Lloyd, R. S., Read, P. J., Moore, I. S., Myer, G. D., & Oliver, J. L. (2022). A novel method to categorize stretch-shortening cycle performance across maturity in youth soccer players. *The Journal of Strength & Conditioning Research*, 36(9), 2573. <https://doi.org/10.1519/JSC.0000000000003900>
- Ramirez-Campillo, R., Sortwell, A., Moran, J., Afonso, J., Clemente, F. M., Lloyd, R. S., Oliver, J. L., Pedley, J., & Granacher, U. (2023). Plyometric-jump training effects on physical fitness and Sport-specific performance according to maturity: A systematic review with meta-analysis. *Sports Medicine - Open*, 9(1), 23. <https://doi.org/10.1186/s40798-023-00568-6>
- Ruf, L., Drust, B., Ehmann, P., Forster, S., Hecksteden, A., & Meyer, T. (2022). Poor reliability of measurement instruments to assess acute responses to load in soccer players irrespective of biological maturity status. *Pediatric Exercise Science*, 34(3), 125–134. <https://journals.humankinetics.com/view/journals/pes/34/3/article-p125.xml>
- Salter, J., Cumming, S., Hughes, J. D., & De Ste Croix, M. (2022). Estimating somatic maturity in adolescent soccer players: Methodological comparisons. *International Journal of Sports Science & Coaching*, 17(1), 11–17. <https://doi.org/10.1177/17479541211020418>
- Sheppard, J., Newton, R., & McGuigan, M. (2007). The effect of accentuated eccentric load on jump kinetics in high-performance volleyball players. *International Journal of Sports Science & Coaching*, 2(3), 267–273. <https://doi.org/10.1260/174795407782233209>
- Street, G., McMillan, S., Board, W., Rasmussen, M., & Heneghan, J. M. (2001). Sources of error in determining countermovement jump height with the impulse method. *Journal of Applied Biomechanics*, 17(1), 43–54. <https://doi.org/10.1123/jab.17.1.43>
- Taber, C., Butler, C., Dabek, V., Kochan, B., McCormick, K., Petro, E., Suchomel, T., & Merrigan, J. (2023). The effects of accentuated eccentric loading on barbell and trap bar countermovement jumps. *International Journal of Strength and Conditioning*, 3(1). <https://journal.iusca.org/index.php/Journal/article/view/213>
- Thomas, C., Comfort, P., Jones, P. A., & Dos'santos, T. (2017). A comparison of isometric midhigh-pull Strength, vertical jump, sprint speed, and change-of-direction speed in academy netball players. *International Journal of Sports Physiology & Performance*, 12(7), 916–921. <https://journals.humankinetics.com/view/journals/ijsp/12/7/article-p916.xml>
- Vanrenterghem, J., De Clercq, D., & Cleven, P. V. (2001). Necessary precautions in measuring correct vertical jumping height by means of force plate measurements. *Ergonomics*, 44(8), 814–818. <https://doi.org/10.1080/00140130118100>
- Wade, L., Needham, L., Evans, M., McGuigan, P., Colyer, S., Cosker, D., & Bilzon, J. (2023). Examination of 2D frontal and sagittal markerless motion capture: Implications for markerless applications. *PLoS One*, 18(11), e0293917. <https://doi.org/10.1371/journal.pone.0293917>
- Wade, L., Needham, L., McGuigan, M. P., & Bilzon, J. L. J. (2022). Backward Double integration is a valid method to calculate maximal and sub-maximal jump height. *Journal of Sports Sciences*, 40(10), 1191–1197. <https://doi.org/10.1080/02640414.2022.2059319>
- Washif, J. A., & Kok, L.-Y. (2022). Relationships between vertical jump metrics and sprint performance, and qualities that distinguish between faster and slower sprinters. *Journal of Science in Sport and Exercise*, 4(2), 135–144. <https://doi.org/10.1007/s42978-021-00122-4>